J MATER SCI **41** (2006) 689–695

Compositional tailoring of the thermal expansion coefficient of tantalum (V) oxide

SUXING WU, HELEN M. CHAN, MARTIN P. HARMER
Center for Advanced Materials and Nanotechnology and Department of Materials Science & Engineering, Lehigh University, Bethlehem, PA 18015

The effect of Al_2O_3 and Nb_2O_5 additions on the microstructure and thermal expansion behavior of tantalum (V) oxide has been studied. Both singly doped and co-doped compositions were examined. Compositions with 3 wt% Al_2O_3 (or greater), contained $AlTaO_4$ as a second phase. Complete solubility was observed for Nb_2O_5 contents in the range 1–5 wt%. It was found that doping with Al_2O_3 results in a decrease of the coefficient of thermal expansion (CTE), such that increasing amounts of Al_2O_3 (1–5 wt%) cause a successive decrease in the CTE value. In the case of Nb_2O_5 additions, the result is an increase in the CTE of the tantalum (V) oxide. However, in the range 1–5 wt% Nb_2O_5, the CTE value is relatively insensitive to the amount of Nb_2O_5 added. Due to the countervailing influences of these two additive oxides, it was demonstrated that co-doping with Al_2O_3 and Nb_2O_5 is an effective strategy for tailoring the CTE of tantalum (V) oxide.

1. Introduction

In terms of ceramic materials, silicon nitride (Si_3N_4) is one of the leading candidates for gas turbine engine applications. A critical issue in this application is the resistance of the material to environmental attack at elevated temperatures [1–4]. The combustion environment normally contains ~10% water vapor, which due to the formation of volatile species, enhances the oxidation process in silicon based materials [2]. Accordingly, there has been strong interest in the development of an environmental barrier coating (EBC) for silicon nitride. A material which has been thought to have good potential as part of an EBC system for Si_3N_4 is tantalum (V) oxide (Ta_2O_5) [5–9]. A critical issue in the development of a successful EBC system is management of the thermal expansion mismatch between the coating and silicon nitride substrate. The objective of the present work is to explore compositional tailoring of the EBC as a means to control and optimize the thermal expansion mismatch.

Ta_2O_5 cannot be used as coating material in the pure state, because it undergoes a series of phase transformations with increasing temperature. Because of the associated volume changes, these transformations are detrimental to the mechanical integrity of the sample [10–13]. In this regard, the most critical phase transition is from the low-temperature orthorhombic (β) phase, to the high-temperature tetragonal (α) phase, which takes place at ~1360°C. We have previously reported that Al_2O_3 is a promising additive for Ta_2O_5, in that for a 3 wt% Al_2O_3 addition, the phase transformation in Ta_2O_5 is effectively suppressed, resulting in crack-free microstructures for samples fired at temperatures up to 1400°C [9]. Preliminary experiments also revealed that the addition of Al_2O_3 results in a lowering of the coefficient of thermal expansion (CTE), whereas the addition of Nb_2O_5 has the reverse effect. The aim of the present work was to explore more fully the effects of these two additive oxides on the thermal expansion behavior. Although there have been several papers describing modeling of multi-phase materials to determine the CTE of the composite [14–16], the authors are not aware of any experimental work on this topic as applied to Ta_2O_5. Moreover, by studying two oxides with opposing influences on the magnitude of the CTE, one aim of the study was to match the expansion behavior of Ta_2O_5 to silicon nitride.

2. Experimental

A series of Ta_2O_5 specimens were prepared with varying amounts of Nb_2O_5 and Al_2O_3 additions. Samples were prepared containing 1, 3 and 5 wt% Nb_2O_5. A second series of samples was also prepared with the same Nb_2O_5 content as above, (i.e., 1, 3 and 5 wt%), but with an additional 3 wt% Al_2O_3. This amount of alumina addition was selected based on previous work which showed that 3 wt% was sufficient to obtain a microcrack-free microstructure

0022-2461 © *2006 Springer Science + Business Media, Inc.*
DOI: 10.1007/s10853-006-6487-x

for sintering at temperatures up to 1400°C [9]. For reference purposes, a single phase sample of $AlTaO_4$ was also processed; this compound occurs as a second phase in Ta_2O_5 – 3 wt% Al_2O_3, and forms when the amount of Al_2O_3 added exceeds the solubility limit [9].

The starting materials were Ta_2O_5 (Alfa Aesar, 99.993 %), γ-Al_2O_3 (Alfa Aesar, 99.98 %, 0.01–0.02 μm) and Nb_2O_5 (99.9985 %, Alfa Aesar) powders. The powder preparation procedure was as follows. First, the various components were attrition milled for 3 h in isopropanol, using 1 mm TZP balls (Tosoh Corporation, Japan) as milling media. The milled mixtures were then dried with a Büchi rotary evaporator, ground with a mortar and pestle, and passed through a 80 mesh sieve to improve homogeneity. The sieved powders were subsequently isostatically compacted into bars (6 × 6 × 30 mm) in a rubber mold at 350 MPa, and fired at 1380°C for 5 h. All heat-treatments were carried out in a box furnace with a heating and cooling rate of 3°C/min. For comparison purposes, samples of undoped Ta_2O_5 were prepared under the same conditions, except these were sintered at 1320°C to avoid the β-to-α phase transformation.

Phase identification for powder and fired samples was carried out using XRD (X-ray diffraction) measurements, which were made using a Rigaku horizontal wide angle goniometer (Model 2154D2). The X-ray source was a Rigaku Rotaflex RU-200B rotating anode generator with a copper anode, operated at 50 kV and 100 mA. The sintered microstructures were characterized by SEM (scanning electron microscopy, JEOL 6300F). Samples for SEM analysis were polished to a 1 μm finish and thermally etched at 1290°C for 15 min.

Thermal expansion data was obtained on bar shaped specimens (4 × 4 × 25 mm) using a Netzsch dilatometer (DIL 402C). The heating cycle consisted of heating up to 1250°C, and then immediately cooling down to room temperature. The heating and cooling rates were 3°C/min.

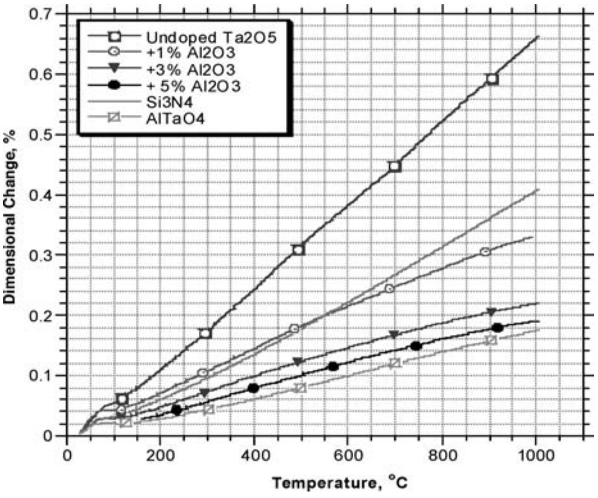

Figure 1 Expansion curves of Si_3N_4, Al_2O_3-doped and undoped Ta_2O_5.

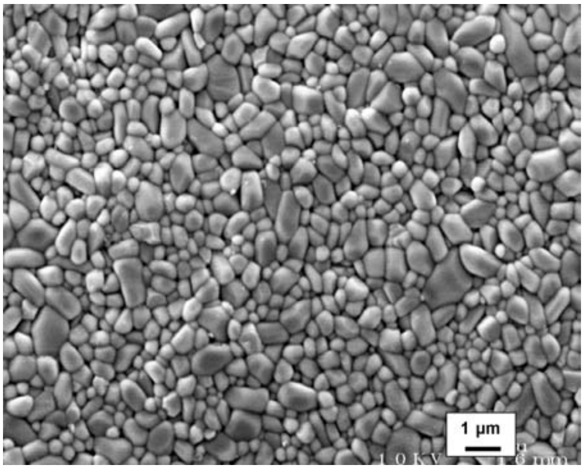

Figure 2 Microstructure of an as-fired surface of $AlTaO_4$ fired at 1380°C for 5 h (SEM).

Values of thermal expansion coefficients of the sintered samples were derived by linear fitting of the recorded data over a temperature span from room temperature up to 1000°C. For reference purposes, the thermal expansion behavior of a Si_3N_4 sample (AS800, provided by the Honeywell Materials Technology Group) was also measured.

3. Results and discussion

3.1. Ta_2O_5-Al_2O_3 System

The expansion curves of Al_2O_3-doped and undoped Ta_2O_5 are shown in Fig. 1. The corresponding data for the Si_3N_4 sample and the $AlTaO_4$ are included for comparison. The thermal expansion coefficients of these materials were derived from Fig. 1, and the values are shown in Table I. The data shows that the undoped Ta_2O_5 exhibits the highest CTE, and that the addition of increasing amounts of Al_2O_3 successively lowers the value of the expansion coefficient. Given that the 3 wt% and 5 wt% Al_2O_3 samples contain $AlTaO_4$ as a second phase, which itself has a CTE which is about a factor of 4 lower than that of Ta_2O_5, this result is expected. It can be seen from Fig. 1 that the expansion curve of the 1 wt% Al_2O_3 sample has a reasonable match with that of Si_3N_4. Unfortunately, however, this

TABLE I Thermal expansion coefficients of Si_3N_4, Al_2O_3-doped and undoped Ta_2O_5

	Thermal expansion coefficient (1/°C)
Si_3N_4 (AS800)	4.33×10^{-6}
Undoped Ta_2O_5	6.72×10^{-6}
Ta_2O_5 doped with 1 wt% Al_2O_3	3.27×10^{-6}
Ta_2O_5 doped with 3 wt% Al_2O_3	2.56×10^{-6}
Ta_2O_5 doped with 5 wt% Al_2O_3	1.95×10^{-6}
$AlTaO_4$	1.84×10^{-6}

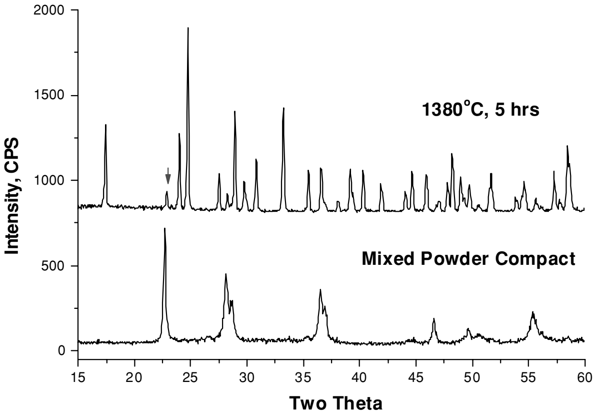

Figure 3 XRD patterns of a γ-Al_2O_3 and Ta_2O_5 powder compact of $AlTaO_4$ composition before and after firing at 1380°C for 5 h. Note that the patterns of the powder mixture were consistent with orthorhombic Ta_2O_5, while those after firing were predominantly orthorhombic $AlTaO_4$.

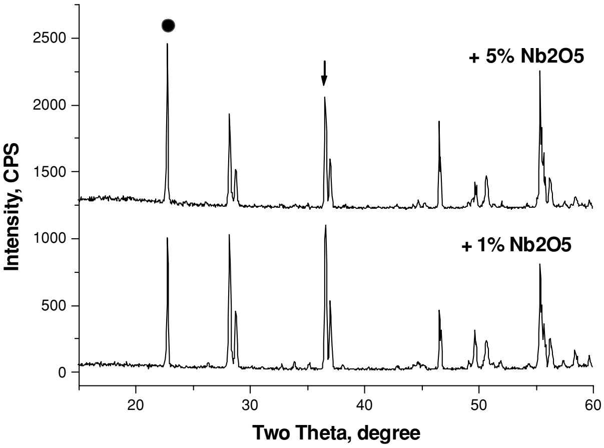

Figure 4 XRD patterns of 1 and 5 wt% Nb_2O_5-doped Ta_2O_5 fired at 1380°C for 5 h.

composition would not be ideal for an EBC, because the additive level is insufficient to suppress the Ta_2O_5 β-to-α phase transformation. A possible strategy, therefore, is to tailor the powder composition to offset the effect of the $AlTaO_4$ second phase on the thermal expansion of Ta_2O_5. It is perhaps worth mentioning that the value for the CTE of undoped tantalum (V) oxide obtained in the present study (6.72×10^{-6}/°C), is higher than values reported previously in the literature [7, 19]. For example, Touloukian *et al.* [19] report a value of 4.0×10^{-6}/°C from 550 to 1200°C. The reason for this discrepancy is not known, but may be related to differences in the temperature range of study, and/or microstructural differences in the Ta_2O_5 samples.

TABLE II Thermal expansion coefficients of 1–5 wt% Nb_2O_5-doped Ta_2O_5

Material	Thermal expansion coefficient (1/°C)
Ta_2O_5 doped with 1 wt% Nb_2O_5	7.78×10^{-6}
Ta_2O_5 doped with 3 wt% Nb_2O_5	7.98×10^{-6}
Ta_2O_5 doped with 5 wt% Nb_2O_5	8.30×10^{-6}

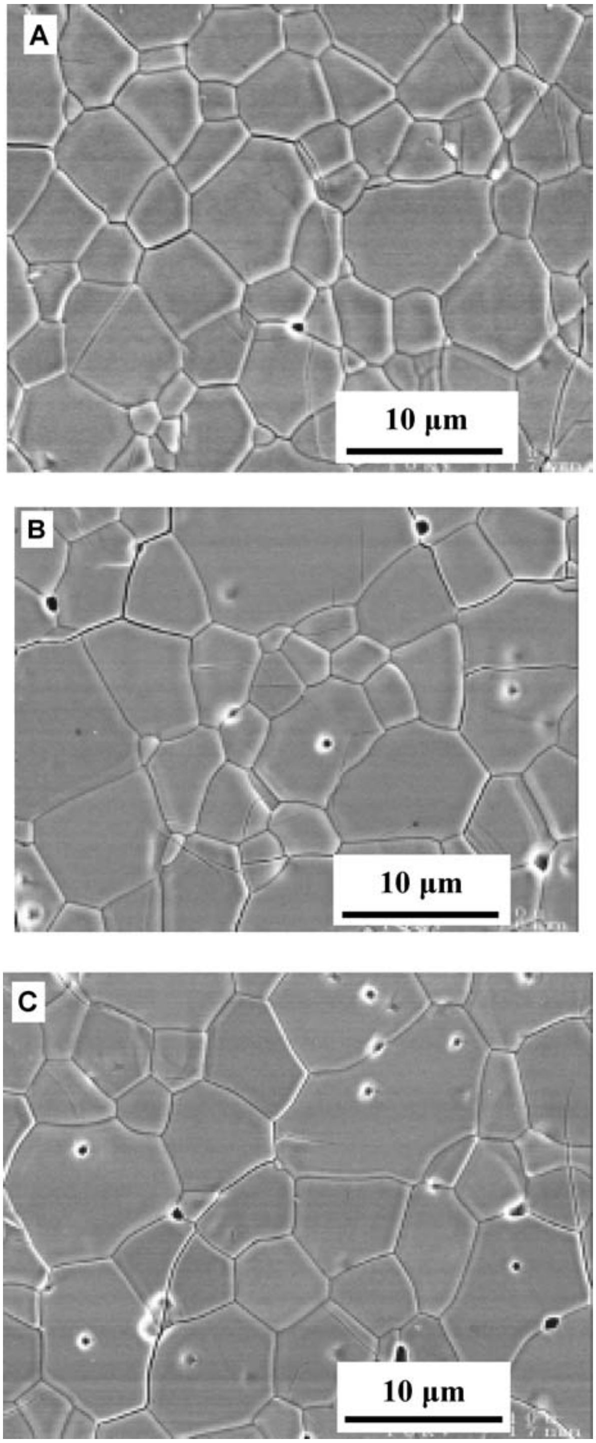

Figure 5 Microstructures of (A) 1, (B) 3 and (C) 5 wt% Nb_2O_5 doped Ta_2O_5 fired at 1380°C for 5 h. Note that microcracking is present in all the samples, indicating partial β-to-α phase transformation took place during firing.

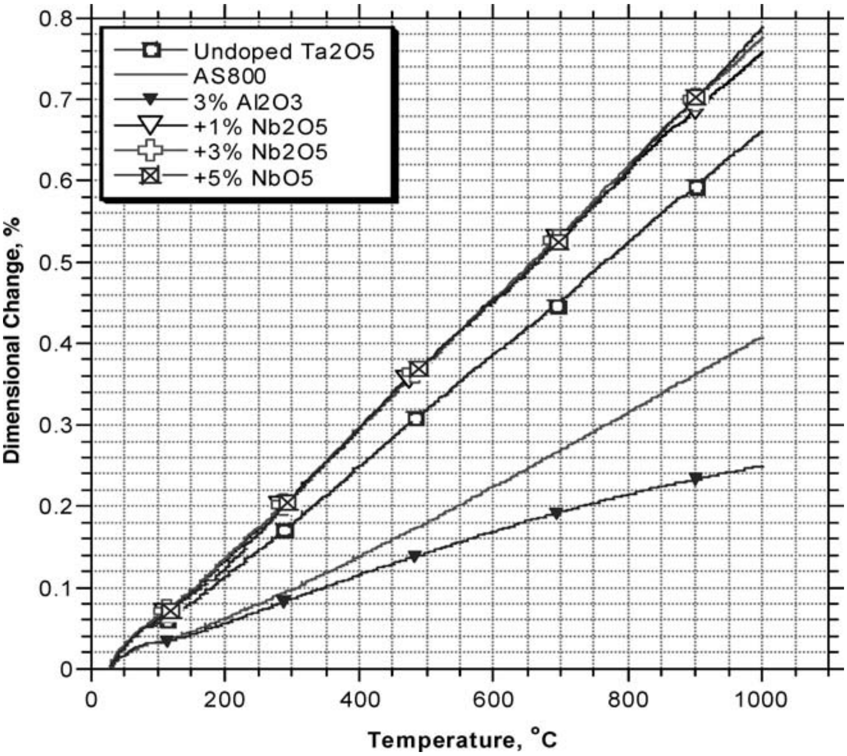

Figure 6 Thermal expansion curves of Ta_2O_5 doped with 1, 3 or 5 wt% Nb_2O_5. Corresponding data for Si_3N_4, $AlTaO_4$, 3 wt% Al_2O_3-doped and undoped Ta_2O_5 are included for comparison.

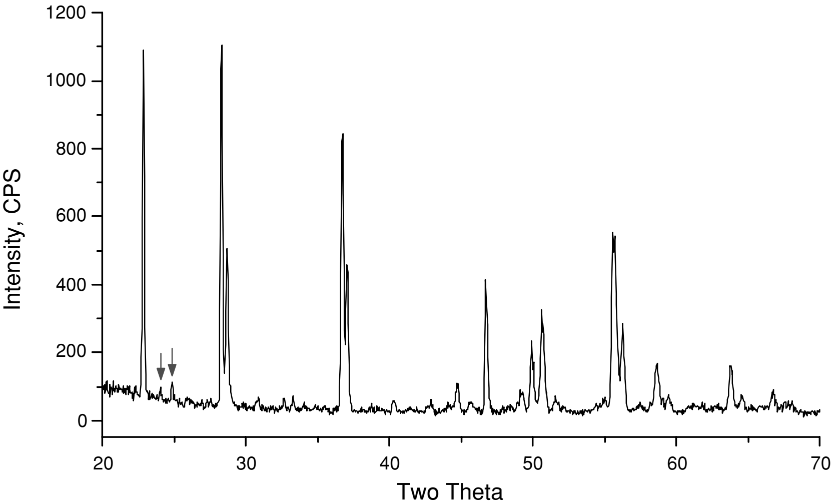

Figure 7 XRD pattern obtained from Ta_2O_5 sample containing 3wt% Al_2O_3 and 5 wt% Nb_2O_5, fired at 1380°C for 5 h. The peaks marked with arrows correspond to $AlTaO_4$, all other peaks correspond to the orthorhombic (ß) phase of Ta_2O_5.

The microstructure of the sintered $AlTaO_4$ sample is shown in Fig. 2. It can be seen that the sintering treatment resulted in a dense, fine-grained microstructure. Examination of this sample using XRD (see Fig. 3) revealed that it was predominantly orthorhombic $AlTaO_4$, with a minor amount (<10%) of residual β-phase Ta_2O_5.

3.2. Ta_2O_5-Nb_2O_5 System

3.2.1. Phase identification and microstructure

Phase identification of the Ta_2O_5 samples containing 1, 3 and 5 wt% Nb_2O_5 was carried out using XRD, and the results are shown in Fig. 4. For ease of comparison, only the XRD patterns from the two end compositions, i.e., 1 and 5 wt% Nb_2O_5 are shown. It can be seen that the XRD patterns of the two samples appear almost identical; and correspond predominantly to the orthorhombic phase of Ta_2O_5. Two of the strongest peaks corresponding to the orthorhombic phase are the (0 1 0) at $2\theta = 22.85^\circ$ (indicated by the solid circle), and the (11 0 2) at $2\theta = 36.61^\circ$ (indicated by the arrow).

The microstructures of the fired samples are depicted in Fig. 5. The presence of microcracks was detected in all the samples, indicating that a partial β-to-α phase transformation had occurred during firing. The absence of second phase particles shows that Nb_2O_5 forms a solid solution with Ta_2O_5 at the additive levels studied. The above observations are consistent with previous phase equilibria studies in the Ta_2O_5-Nb_2O_5 system [17, 18].

3.2.2. Thermal expansion studies on Ta_2O_5-Nb_2O_5 system

The thermal expansion curves of the Nb_2O_5-doped Ta_2O_5 samples are shown in Fig. 6. The expansion curves of the $AlTaO_4$, 3 wt% Al_2O_3-doped Ta_2O_5 and AS800 Si_3N_4 are also plotted for comparison. It can be seen that the addition of 1 wt% Nb_2O_5 to Ta_2O_5 results in an increase in the thermal expansion coefficient. With increasing Nb_2O_5 content, there is little further change, so that the curves for the three Nb_2O_5 - doped compositions are practically superposed. This result is also apparent from Table II, where it can be seen that the calculated values of CTE differ by less than 3%. The above results suggest a promising approach to modifying the thermal expansion behavior of Al_2O_3-doped Ta_2O_5 to match that of AS800 Si_3N_4, i.e., co-doping with Nb_2O_5.

3.3. Ta_2O_5 co-doped with Al_2O_3 and Nb_2O_5

3.3.1. Phase identification and microstructure

Analysis of the co-doped Ta_2O_5 samples using XRD revealed that for the Ta_2O_5-3 wt% Al_2O_3-x wt% Nb_2O_5 compositions, where $x = 1$, 3 or 5, the patterns were very similar. Aside from two small peaks which correspond to the $AlTaO_4$ second phase, the peak positions and intensities were completely consistent with data which would be obtained for orthorhombic (β) Ta_2O_5. Fig. 7 shows a XRD pattern which is representative of this series of compositions.

The microstructures of the fired samples are shown in Fig. 8. It can be seen that some degree of microcracking occurred in all samples, indicating that a partial β-to-α phase transformation took place during firing at 1380°C. This contrasts with the results for Al_2O_3 additions only, where it was observed that 3 wt% Al_2O_3 was sufficient to stabilize the β structure at this temperature.

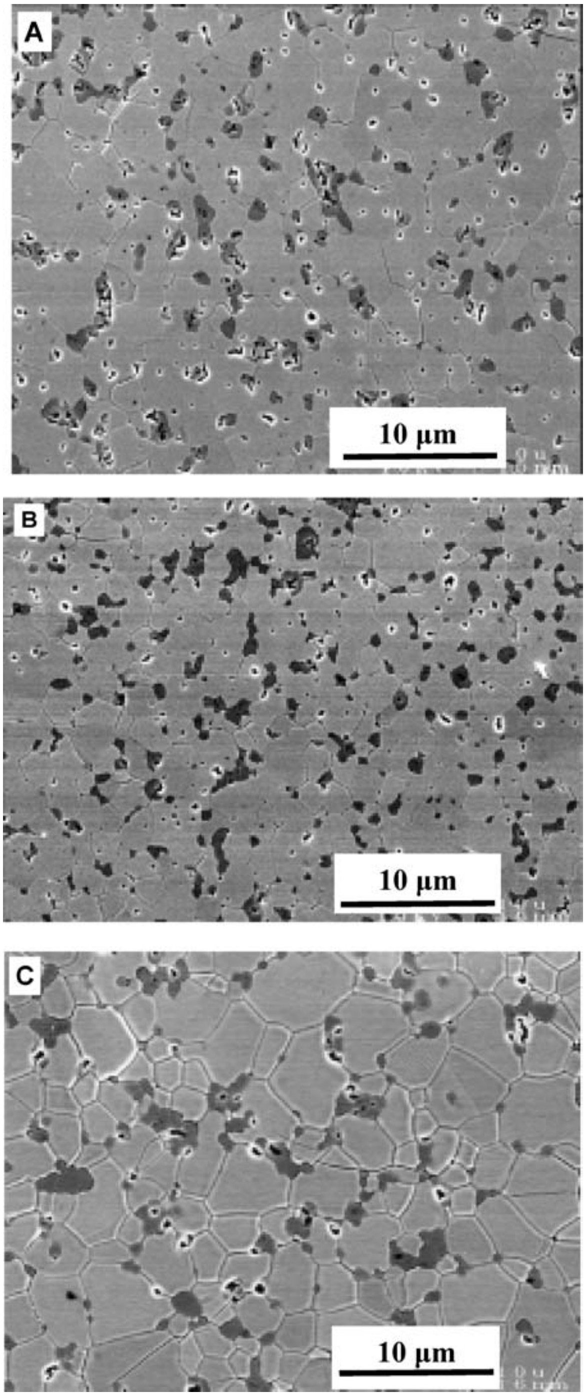

Figure 8 Microstructures of Ta_2O_5 doped with 3% Al_2O_3 and various amount of Nb_2O_5: (A) 1%; (B) 3%; (C) 5%. Samples were fired at 1380°C for 5 h.

The reason for the difference in behavior is not fully understood, and requires further study. One possibility is that the effect of the Nb_2O_5 is to negate the beneficial influence of Al_2O_3 on the transition temperature. Alternately, we may speculate that the presence of dissolved Nb_2O_5

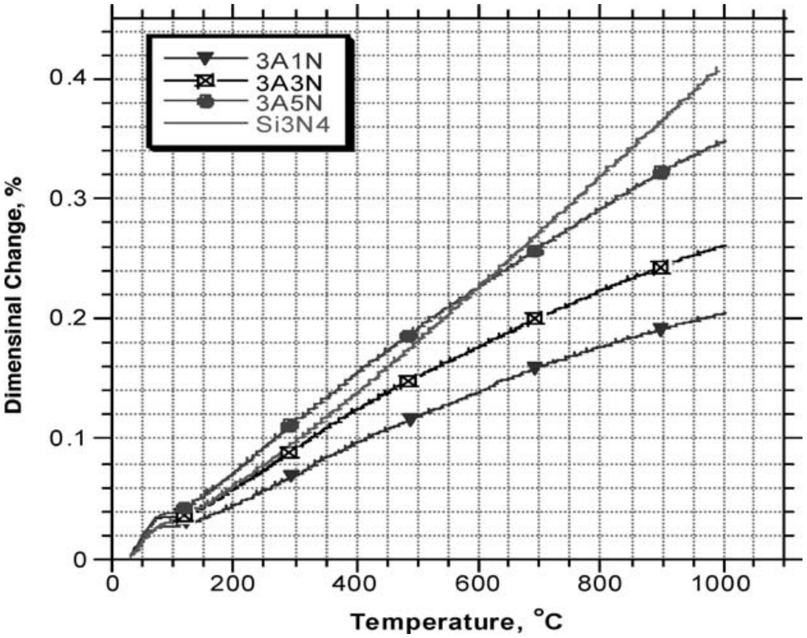

Figure 9. Thermal expansion behavior of Ta_2O_5 co-doped with 3 wt% Al_2O_3 and 1, 3 or 5 wt% Nb_2O_5. Corresponding data for $AlTaO_4$ and AS800 Si_3N_4 are included for comparison.

in the Ta_2O_5 lattice reduces the solubility of Al_2O_3, and there is now insufficient alumina addition to completely suppress the transformation.

3.3.2. Thermal expansion studies on $Ta_2O_5/Al_2O_3/Nb_2O_5$ system

The thermal expansion curves of Ta_2O_5 co-doped with 3 wt% Al_2O_3 and 1–5 wt% Nb_2O_5 are presented in Fig. 9, and the corresponding CTE values are given in Table III. The results show that the further addition of Nb_2O_5 to the Al_2O_3 containing compositions resulted in an overall increase in the CTE. Given that originally, the CTE of the Ta_2O_5- 3 wt% Al_2O_3 composition was *below* that of the silicon nitride, this co-doping approach was successful in achieving a match with the thermal expansion coefficient of AS800 Si_3N_4. It can be seen from Fig. 9 that of the samples studied, the closest match is obtained with the Ta_2O_5-3 wt% Al_2O_3 – 5 wt% Nb_2O_5 composition.

TABLE III Thermal expansion coefficients of Ta_2O_5, $AlTaO_4$ and AS800 Si_3N_4 ceramics in a temperature range up to 1000°C

Material	Thermal expansion coefficient (1/°C)
Si_3N_4 (AS800)	4.33×10^{-6}
Ta_2O_5 doped with 3 wt% Al_2O_3 and 1 wt% Nb_2O_5	2.00×10^{-6}
Ta_2O_5 doped with 3 wt% Al_2O_3 and 3 wt% Nb_2O_5	2.54×10^{-6}
Ta_2O_5 doped with 3 wt% Al_2O_3 and 5 wt% Nb_2O_5	4.24×10^{-6}

4. Summary

The addition of Al_2O_3 and Nb_2O_5 can modify the thermal expansion coefficient of tantalum (V) oxide (Ta_2O_5). Doping with Al_2O_3 results in a decrease of the CTE, such that increasing amounts of Al_2O_3 cause a successive decrease in the CTE value. This is attributed to the formation of a second phase, $AlTaO_4$, which has a lower CTE than Ta_2O_5. In the case of Nb_2O_5 additions, the result is an increase in the CTE of the tantalum (V) oxide. However, in the range 1–5 wt%, the Nb_2O_5 forms a solid solution, and the CTE value is relatively insensitive to the amount of Nb_2O_5 added. Due to the countervailing influences of these two additive oxides, it was demonstrated that co-doping with Al_2O_3 and Nb_2O_5 is an effective strategy for tailoring the CTE of tantalum (V) oxide. From the standpoint of potential applications of Ta_2O_5 as part of an EBC system for silicon nitride, closest matching was obtained with the composition Ta_2O_5 – 3 wt% Al_2O_3 – 5 wt% Nb_2O_5.

Acknowledgements

This work was supported by the U.S. Department of Energy (Contract DE-FC02-01CH11086). The AS800 silicon nitride sample was kindly provided by J.W. Guiheen and C.-W. Li at Honeywell Corp.

References

1. N. S. JACOBSON, *J. Am. Ceram. Soc.* **76** (1995) 1297.
2. E. J. OPILA, *ibid.* **86** (2003) 1238.

3. R. CHAIM, S. ALMALEH-ROCKMAN and L. GAL-OR, *ibid.* **77** (1994) 3202.
4. H. DU, R. E. TRESSLER and C. G. PANTONO, *J. Electrochem. Soc.* **136** (1989) 1527.
5. S. SHANMUGHAM, M. HENDERICK, N. RICHARDS and M. OJACA, *J. Mater. Sci.* **39** (2004) 377.
6. M. MOLDAVAN, C. M. WEYANT, D. L. JOHNSON and K. FABER, *J. Thermal Spray Technol.* **13** (2004) 51.
7. Y. W. BAE, W. Y. LEE and D. P. STINTON, *J. Am. Ceram. Soc.* **78** (1995) 1927.
8. A. REISMAN, F. HOLZBERG, M. BERKENLIT and M. BERRY, *J. Am. Chem. Soc.* **78** (1956) 4514.
9. S. WU, H. M. CHAN and M. P. HARMER, *J. Am. Ceram. Soc.*, in press.
10. O. YAMAGUCHI, D. TOMIHISA, M. SHIRAI and K. SHIMIZU, *ibid.* **71** (1988) C-260.
11. O. YAMAGUCHI, D. TAMIHISA, T. UEGAKI and K. SHIMIZU, *ibid.* **70** (1987) C-335.
12. J. L. WARING and R. S. ROTH, *J. Res. Natl. Bur. Stand.* **72A** (1968) 175.
13. R. S. ROTH, J. L. WARING and W. S. BROWER, *J. Res. Natl. Bureau Stand. - A. Phys. and Chem.* **74A** (1970) 477.
14. S. FREOUR, D. GLOAGUEN, M. FRANCOIS and R. GUILLEN, *Mater. Sci. Forum* **426–432** (2003) 2083.
15. C. H. HSUEH, P. F. BECHER and E. Y. SUN, *J. Mater. Sci.* **36** (2001) 255.
16. Y.-S. LEE, M. N. GUNGOR, T. J. BATT and P. K. LIAW, *Mater. Sci. Eng.* **A 145** (1991) 37.
17. A. REISMAN and F. HOLTZBERG, *High Temp. Oxides* **2** (1970) 217.
18. G. P. MOHANTY, L. J. FIEGEL and J. H. HEALY, *J. Phys. Chem.* **68** (1964) 208.
19. Y. S. TOULOUKIAN, R. K. KIRBY, R. E. TAYLOR and T. Y. R. LEE, "Thermal Expansion, Nonmetallic Solids." (Plenum, New York, 1977) p. 374.